Article

Journal of Vibration and Control
1–11

DOI: 10.1177/1077546315623147
jvc.sagepub.com
SAGE

Vehicle axle identification using wavelet analysis of bridge global responses

Yang Yu[1], CS Cai[1] and Lu Deng[2]

Abstract

Bridge weigh-in-motion (BWIM) technique uses an instrumented bridge as a weighing scale to estimate vehicle weights. Traditional BWIM systems use axle detectors placed on the road surface to identify vehicle axles. However, the axle detectors have poor durability due to the direct exposure to the traffic. To resolve this issue, a free-of-axle-detector (FAD) algorithm, which eliminates the use of axle detectors, was proposed. As a further improvement to simplify the BWIM systems, the concept of nothing-on-road (NOR) BWIM was recently introduced. The axle identification method proposed in this paper is an attempt to achieve the NOR BWIM, i.e., using bridge global responses to identify vehicle axles. Wavelet analysis is applied to extract the axle information from the global responses. This allows the BWIM technique to be achieved with only weighing sensors. Numerical simulations are conducted using three-dimensional vehicle and bridge models and the effect of several parameters, including sampling frequency, road surface condition and measurement noise on the identification accuracy is investigated. The results demonstrate that the proposed identification method using wavelet analysis can accurately identify vehicle axles, except for cases where the road surface condition is rough or measurement noises exceed certain levels.

Keywords

Bridge weigh-in-motion (BWIM), vehicle axle identification, wavelet analysis, global response, nothing-on-road (NOR)

1. Introduction

Bridge weigh-in-motion (BWIM) is a recently developed technology that aims at identifying vehicle weights using an instrumented bridge as the weighing scale. Compared to the traditional pavement-based WIM techniques, the BWIM technique has several advantages: (1) a BWIM system is more durable than a pavement-based WIM system since most sensors are not directly exposed to traffic; (2) the installation of a BWIM system is easy and safe as it can be done without interrupting the traffic and (3) a BWIM system is potentially more accurate than a pavement-based WIM system since it records the complete time history of the bridge response (O'Brien et al., 1999). These advantages have made the BWIM systems a cost-effective alternative to the pavement-based WIM systems and a potential tool for truck overweight enforcement.

Axle detection is an indispensable part of the BWIM systems. In traditional BWIM systems, the sensors can be classified into two types, i.e., the weighing sensors and axle detectors. The weighing sensors measure the bridge global responses, usually in terms of bending strains, due to the vehicle loading and thus they are usually installed at locations of most pronounced responses, e.g., the mid-span of the bridge. Axle detectors are typically placed on the road surface to identify the vehicle speed and axle spacing which are then used as inputs to the BWIM algorithm to calculate axle weights (Moses, 1979). While the method using axle detectors is very accurate, the durability of the detectors becomes a concern. In an effort to address this concern, a free-of-axle-detector (FAD) algorithm was developed in the WAVE project (WAVE, 2001). The concept of the FAD algorithm is to replace the traditional axle detectors on the road surface by placing the FAD sensors underneath the bridge to measure the

[1]Department of Civil and Environmental Engineering, Louisiana State University, Baton Rouge, Louisiana, USA
[2]College of Civil Engineering, Hunan University, Changsha, Hunan, China

Received: 14 July 2015; accepted: 25 November 2015

Corresponding author:
CS Cai, Department of Civil and Environmental Engineering, Louisiana State University, Baton Rouge, Louisiana 70803, USA.
Email: cscai@lsu.edu

bridge local responses. An important feature of the FAD sensors is that they show a sharp peak when an axle is present above the sensor location. The application of the FAD algorithm eliminates the use of axle detectors that have poor durability. However, it still requires the FAD sensors solely for the purpose of identifying the vehicle velocity and axle spacing. Also, the FAD algorithm is not applicable to all types of bridges as it imposes certain restrictions, such as thin superstructure, short span, etc (WAVE, 2001).

Recently, the concept of a nothing-on-road (NOR) BWIM system was proposed. The goal of the NOR BWIM is to free the use of axle detectors as well as FAD sensors and to directly employ the strain signal obtained from weighing sensors to identify the vehicle speed and axle spacing. This will be a very attractive feature for commercial BWIM systems since it reduces the number of sensors and thus the cost of the system, making the installation even easier. However, the strain signal of weighing sensors corresponds to the global response of the bridge, which means that a direct identification from the signal would be very difficult. Therefore, a proper signal processing technique needs to be employed to extract the axle information from the strain signal.

Wavelet analysis is a recently developed technique that provides a powerful tool to solve many difficult engineering problems. This exciting new method has been applied to many fields such as signal processing, data compression, computer graphics, etc. Nevertheless, the study on the use of wavelet analysis in the identification of vehicle axles has been very limited. Dunne et al. (2005) first proposed using wavelet transformation to identify closely-spaced axles from the FAD signals. Chatterjee et al. (2006) conducted a further study to explore the possibility of using wavelet transformation of the strain signal to identify the vehicle axles. In their study, a numerical simulation was carried out on a simply supported beam and field testing was conducted on a short box culvert. The results showed that wavelet analysis is able to identify the vehicle velocity and axle spacing with a reasonable accuracy. However, the beam model seems overly simple to accurately represent the behavior of the bridge. Moreover, the box culvert used in their study is a very simple structure and it has been reported that for these types of structures, the dynamic effect caused by a vehicle is basically negligible (Quilligan, 2003). Besides, in their field test, the obtained strain signals already have relatively sharp peaks corresponding to some axles due to the fact that the instrumented superstructure is very thin. Thus, the identification was actually achieved through the wavelet analysis of bridge local responses rather than the global responses.

The objective of this paper is to employ the wavelet technique to identify vehicle axles from the signals of weighing sensors, i.e., the bridge global responses, which give no direct information with respect to the vehicle axles. A brief introduction on the wavelet theory is first given. Numerical simulations are then carried out on a multi-girder bridge with different trucks traveling at different speeds and a continuous wavelet transformation is then used to extract the information of vehicle axles from the bridge global responses. A parametric study is finally conducted to investigate the effect of several parameters including the sampling frequency, road surface condition and measurement noise on the identification accuracy.

2. Wavelet theory

Fourier analysis allows the frequency information being extracted from the signal presented in the time domain. However, the time information is lost during the Fourier transformation (FT), i.e., it gives no information on the time occurrence of certain frequency components of the signal. In this sense, Fourier analysis is only suitable for stationary signals or cases where the time information is not of interest. To overcome this drawback, short-time Fourier analysis (STFT) was proposed (Gabor, 1946). The idea of the STFT is to divide the signal into many intervals and the signal in each small interval is assumed to be stationary. In this case, FT can be carried out at each time interval and a time-frequency representation of the signal can be obtained. However, the STFT is still not the perfect solution to analyze non-stationary signals since it has a fixed resolution, i.e., a satisfactory resolution with respect to both time and frequency cannot be achieved at the same time. Wavelet transformation was then developed on this basis to provide a multiresolution analysis of the signal. The purpose of the wavelet transformation is to expand the signal in terms of wavelets which are generated from the transformations, including dilations and translations, of the wavelet function, i.e., a compactly supported function that is also known as the mother wavelet. An important feature of the wavelet transformation is that the width of the window can be changed to adapt to different frequency components of the signal. Therefore, wavelet analysis is very effective in analyzing non-stationary signals.

The continuous wavelet transformation (CWT) of a signal is defined as:

$$W_\psi(a,b) = \frac{1}{\sqrt{a}}\int_{-\infty}^{\infty} s(t)\psi\left(\frac{t-b}{a}\right)\mathrm{d}t \tag{1}$$

where a is the scaling factor; b is the shifting factor; $s(t)$ is the signal as a function of time; and $\psi(t)$ is the so-called mother wavelet that must satisfy the following criterion:

$$\int_{-\infty}^{\infty} \frac{\left|\hat{\psi}(\omega)\right|^2}{|\omega|} \mathrm{d}\omega < \infty \tag{2}$$

where $\hat{\psi}(\omega)$ is the Fourier transformation of $\psi(t)$. This is known as the admissibility condition which implies $\hat{\psi}(0) = 0$. If we define $\psi_{a,b}(t)$ as:

$$\psi_{a,b}(t) = \frac{1}{\sqrt{a}} \psi\left(\frac{t-b}{a}\right) \tag{3}$$

then equation (1) can be rewritten as the inner product of the signal $s(t)$ and $\psi_{a,b}(t)$ as:

$$W_{\psi}(a,b) = \int_{-\infty}^{\infty} s(t)\psi_{a,b}(t)\mathrm{d}t \tag{4}$$

In terms of the application in the identification of vehicle axles, the presence or absence of a vehicle axle will cause a sudden change of the slope of the strain signal. While this abrupt change is very difficult to directly observe, a wavelet analysis may be able to amplify these slope discontinuities in the form of sharp peaks in the transformed signal. In the present study, the Morlet wavelet is used to conduct the CWT after comparing the performance with several alternatives such as the reverse biorthogonal wavelets and Daubechies wavelets. The Morlet wavelet can be considered as a modulated Gaussian wave formation. It has a good locality property in both the time and frequency domains. Technically, the Morlet wavelet is complex-valued. However, in many applications, only the real part is used. The complex version is more well-known as the Gabor wavelet. A figure representation of the Morlet wavelet used in this study is shown in Figure 1 and the wavelet function is given as:

$$\psi(t) = e^{-\frac{t^2}{2}} \cos(5t) \tag{5}$$

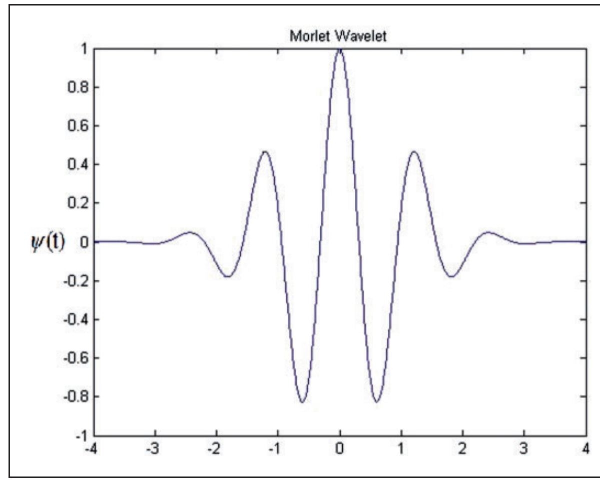

Figure 1. The Morlet wavelet.

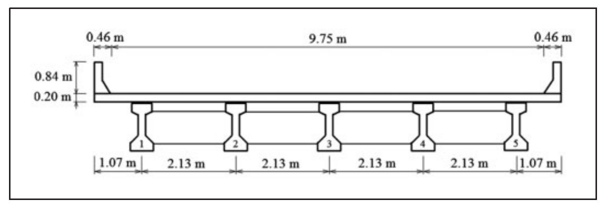

Figure 2. Cross-section of the bridge.

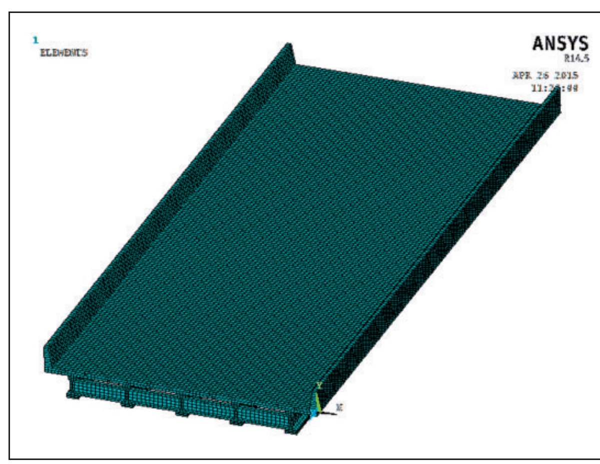

Figure 3. Finite element model of the bridge.

3. Numerical simulations

3.1. Bridge model

In the present study, a simply-supported multi-girder concrete bridge was adopted for the simulation. As a good representative of highway bridges, the selected bridge was designed according to AASHTO standard specification (AASHTO, 2002) and the bridge span length is 24.38 meters (80 ft). The bridge has a uniform cross-section consisting of five identical I-girders and three diaphragms located at the two ends and middle. The cross-section of the bridge is shown in Figure 2. The bridge was modeled with the ANSYS software using solid elements (with three translational degrees-of-freedom at each node) to predict the fundamental dynamic characteristics including the natural frequencies and mode shapes. Figure 3 shows the finite element model of the bridge. The fundamental frequency of the bridge was found to be 3.46 Hz.

3.2. Vehicle Model

In this study, four typical highway trucks with different axle configurations as listed in Table 1 were employed. In the numerical simulation, the truck was modeled using spring-dashpot systems. The vehicle bodies (tractor and trailer) were represented by rigid bodies with mass and three DOFs, i.e., the vertical displacement, pitching rotation, and rolling rotation. The connection between the tractor and trailer is modeled as a pinned connection, i.e., the tractor and trailer have equal vertical displacement at the connection. Each wheel was represented by a lumped mass with one DOF, i.e., the vertical displacement. An analytical model of Truck 2 is shown in Figure 4.

3.3. Vehicle-bridge Interaction

The interaction between the bridge and vehicle can be solved by either an iterative procedure (Broquet et al., 2004) or a coupled approach (Deng and Cai, 2010). In this study, the coupled approach was used. The equations of motion for the vehicle and bridge can be written in matrix forms as:

$$[M_v]\left\{\ddot{d}_v\right\} + [C_v]\left\{\dot{d}_v\right\} + [K_v]\{d_v\} = \{F_G\} + \{F_v\} \tag{6}$$

Table 1. Axle configurations of truck models.

Truck Number	Number of axles	Axle spacing: First to second (m)	Second to third (m)	Third to fourth (m)	Fourth to fifth (m)
1	2	6.25	N.A.	N.A.	N.A.
2	3	4.27	4.27	N.A.	N.A.
3	3	4.94	1.40	N.A.	N.A.
4	5	8.00	5.00	2.00	5.00

$$[M_b]\left\{\ddot{d}_b\right\} + [C_b]\left\{\dot{d}_b\right\} + [K_b]\{d_b\} = \{F_b\} \tag{7}$$

where $[M_v]$, $[C_v]$, and $[K_v]$ = the mass, damping, and stiffness matrices of the vehicle, respectively; $[M_b]$, $[C_b]$, and $[K_b]$ = the mass, damping, and stiffness matrices of the bridge, respectively; $\{d_v\}$ and $\{d_b\}$ = the displacement vector of the vehicle and bridge, respectively; $\{F_G\}$ = the gravity force vector of the vehicle; and $\{F_v\}$ and $\{F_b\}$ = the wheel-road contact force vectors acting on the vehicle and bridge, respectively, and they can be expressed as:

$$\{F_b\} = -\{F_v\} = [K_l]\{\Delta_l\} + [C_l]\{\dot{\Delta}_l\} \tag{8}$$

where $[K_l]$ and $[C_l]$ = coefficients of the vehicle lower spring and damper, respectively; Δ_l is the deformation of the lower spring of the vehicle which can be obtained from the displacement relationship:

$$Z_a = Z_b + \Delta_l + r(x) \tag{9}$$

where Z_a is the vehicle axle suspension displacement; Z_b is displacement of the bridge at the wheel-road contact point; and r(x) is the road surface elevation as a function of the vehicle position.

Based on the interaction force relationship and displacement relationship at the contact points, namely, equation (8) and equation (9), the two equations of motion for the vehicle and bridge can be combined into one coupled equation:

$$\begin{bmatrix} M_b & \\ & M_v \end{bmatrix}\begin{Bmatrix} \ddot{d}_b \\ \ddot{d}_v \end{Bmatrix} + \begin{bmatrix} C_b + C_{b-b} & C_{b-v} \\ C_{v-b} & C_v \end{bmatrix}\begin{Bmatrix} \dot{d}_b \\ \dot{d}_v \end{Bmatrix} + \begin{bmatrix} K_b + K_{b-b} & K_{b-v} \\ K_{v-b} & K_v \end{bmatrix}\begin{Bmatrix} d_b \\ d_v \end{Bmatrix} = \begin{Bmatrix} F_{b-r} \\ F_{v-r} + F_G \end{Bmatrix} \tag{10}$$

where C_{b-b}, C_{b-v}, C_{v-b}, K_{b-b}, K_{b-v}, K_{v-b}, F_{b-r}, and F_{b-r} are the interaction terms caused by the contact

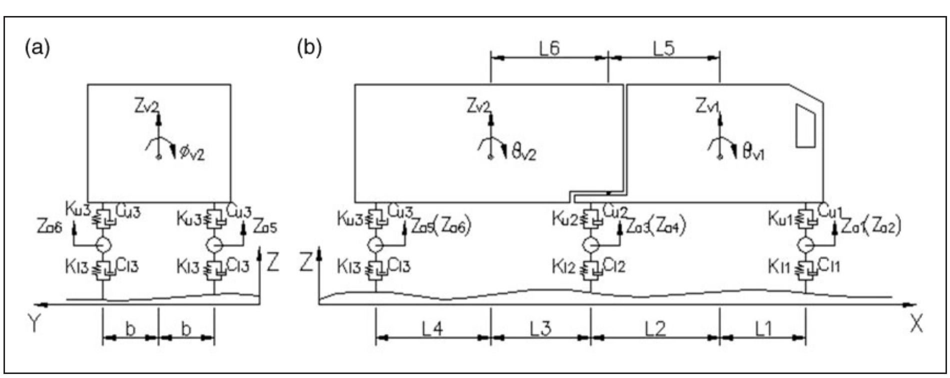

Figure 4. Analytical model of Truck 2. (a) Back view and (b) Side view.

forces. As the vehicle moves across the bridge, the positions of contact points change and so do the contact forces. Thus, the interaction terms are time-dependent terms and will change as the vehicle moves across the bridge.

In order to reduce the size of the matrices and save calculation efforts, the modal superposition technique was adopted and the bridge displacement vector $\{d_b\}$ in equation (10) can therefore be expressed as:

$$\{d_b\} = \left[\{\Phi_1\} \quad \{\Phi_2\} \ldots \{\Phi_m\}\right]\left\{\xi_1 \quad \xi_2 \cdots \xi_m\right\}^T = [\Phi_b]\{\xi_b\} \tag{11}$$

where m = the total number of modes considered for the bridge; $\{\Phi_i\}$ and ξ_i = the ith mode shape of the bridge and the ith generalized modal coordinate, respectively. If each mode shape is normalized such that $\{\Phi_i\}^T[M_b]\{\Phi_i\} = 1$ and $\{\Phi_i\}^T[K_b]\{\Phi_i\} = \omega_i^2$ and the damping matrix $[C_b]$ in equation (7) is assumed to be equal to $2\omega_i\eta_i[M_b]$, where ω_i and η_i = the natural circular frequency and the percentage of the critical damping of the ith mode of the bridge, respectively, then equation (10) can be simplified as:

$$\begin{aligned} &\begin{bmatrix} I & \\ & M_v \end{bmatrix}\begin{Bmatrix} \ddot{\xi}_b \\ \ddot{d}_v \end{Bmatrix} + \begin{bmatrix} 2\omega_i\eta_i I + \Phi_b^T C_{b-b}\Phi_b & \Phi_b^T C_{b-v} \\ C_{v-b}\Phi_b & C_v \end{bmatrix}\begin{Bmatrix} \dot{\xi}_b \\ \dot{d}_v \end{Bmatrix} \\ &\quad + \begin{bmatrix} \omega_i^2 I + \Phi_b^T K_{b-b}\Phi_b & \Phi_b^T K_{b-v} \\ K_{v-b}\Phi_b & K_v \end{bmatrix}\begin{Bmatrix} \xi_b \\ d_v \end{Bmatrix} = \begin{Bmatrix} \Phi_b^T F_{b-r} \\ F_{v-r} + F_G \end{Bmatrix} \end{aligned} \tag{12}$$

The coupled equation (12) contains only the modal properties of the bridge and the mechanical parameters of the vehicles. As a result, the complexity of solving the coupled equations was significantly reduced. A computer program was developed in the MATLAB environment to solve equation (12) in the time domain using the fourth-order Runge-Kutta method. After obtaining the displacement responses of the bridge $\{d_b\}$, the strain responses can be obtained through:

$$\{\varepsilon\} = [B]\{d_b\} \tag{13}$$

where $[B]$ = the strain-displacement relationship matrix assembled with the x, y, and z derivatives of the element shape functions. The $[B]$ matrix depends on the type of finite elements employed and can be derived following the standard finite element formulation procedure.

3.4. Simulation results

In the numerical simulation, each of the four highway trucks are set to cross the bridge at three constant speeds, i.e., 10 m/s, 20 m/s and 30 m/s in lane 2 and Figure 5 shows the transverse position of the vehicle on the bridge. In a commercial BWIM system, five weighing sensors would be installed underneath the five girders at the mid-span to measure the global responses of the bridge, i.e., longitudinal strain responses, and at least four FAD sensors (two for each lane) would be installed underneath the bridge slab to identify the vehicle axles. In this study, as an attempt to achieve the NOR BWIM without FAD sensors, the strain signal of the weighing sensor installed on the girder directly beneath the vehicle trajectory, i.e., Girder 4, is used for the axle identification.

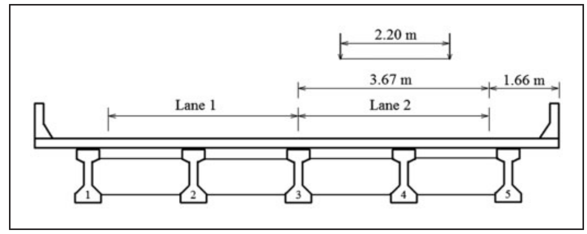

Figure 5. Transverse position of the vehicle on the bridge.

Figure 6 shows the typical time histories of the strain response of Girder 4 corresponding to Trucks 2 and 4 traveling at 20 m/s and 10 m/s under a smooth road surface, respectively. A sampling frequency of 200 Hz is used. From the strain response histories, it can be seen that there is no obvious information on the presence of vehicle axles. This is understandable since the longitudinal strain responses of girders are the global responses of the bridge and they are not sensitive to the presence of axle loads. Nevertheless, as discussed before, the details of the original strain signals still contain the information of vehicle axles. Therefore, a CWT is conducted on the strain signals and the results are presented in Figure 6. The plotted wavelet coefficients are chosen at the scale of 14. As can be seen, the transformed signals have several pronounced peaks. These sharp peaks correspond to vehicle axles entering or exiting the bridge. For the three-axle truck, i.e., Truck 2, the first three peaks correspond to the three axles entering the bridge and the last three peaks correspond to the three axles exiting the bridge. Again, the same feature was also observed for the transformed signal for Truck 4, i.e., the five-axle truck.

Since the span length of the bridge is already known, the vehicle speed can be calculated from the time difference between each vehicle axle entering and exiting the bridge. Once the vehicle speed is known, the time difference between vehicle axles can be used to obtain the axle spacing of the truck. For the signals shown in Figure 6, the velocity and two axle spacings of Truck 2 were calculated as 19.85 m/s, 4.22 m and 4.27 m, respectively, and the velocity and four axle spacings

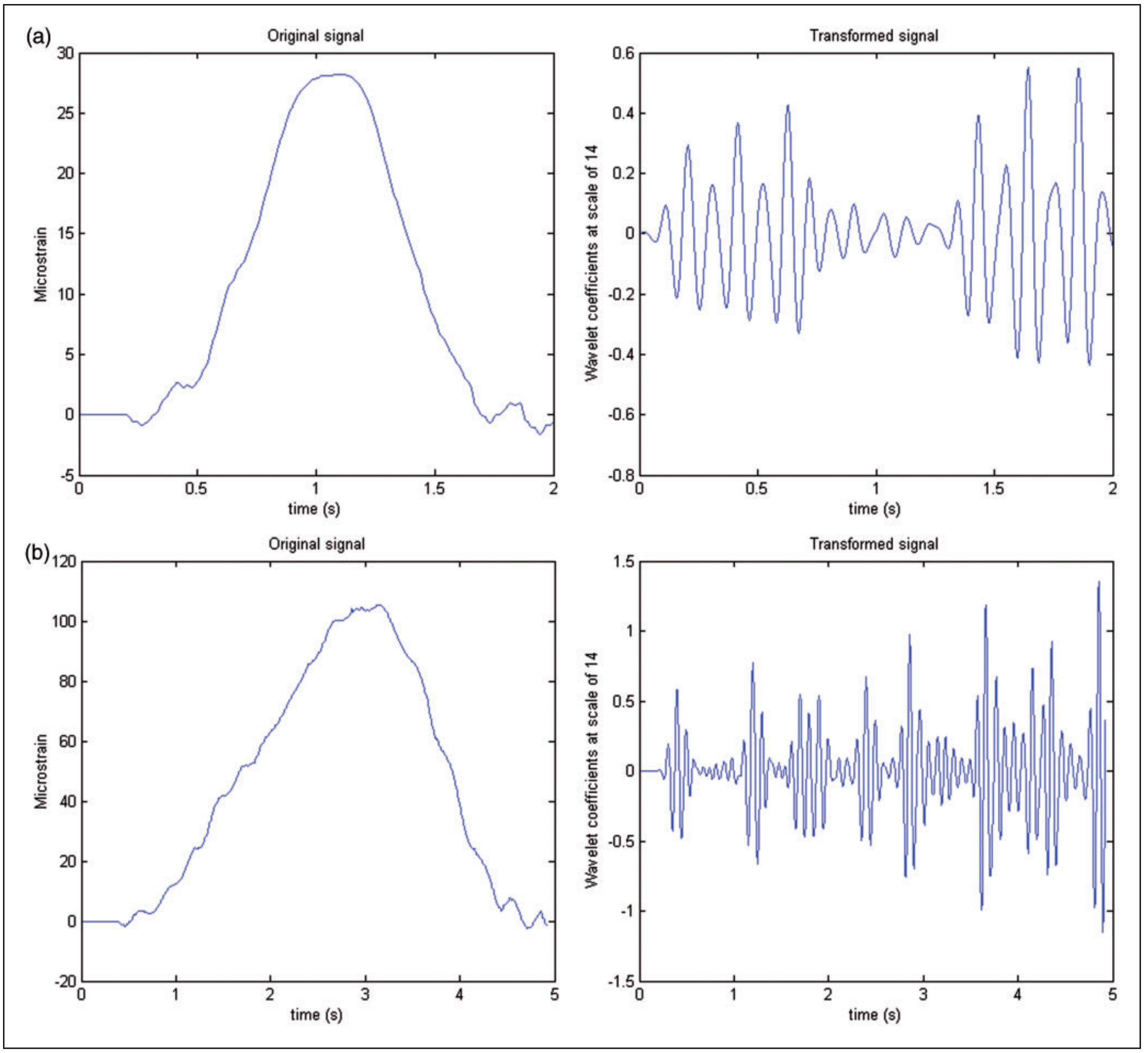

Figure 6. Typical strain signals and corresponding wavelet transformations at scale of 14: (a) Truck 2 (3-axle) traveling at 20 m/s and (b) Truck 4 (5-axle) traveling at 10 m/s.

of Truck 4 were calculated as 9.92 m/s, 7.96 m, 4.94 m, 1.99 m and 4.94 m, respectively. Compared to the true values given in Table 1, the identified results are found to be very accurate.

The identification results for all considered cases are tabulated in Table 2. To better examine the accuracy of identification, the identification error is defined as:

$$\text{Identification Error} = \left| \frac{P_{iden} - P_{true}}{P_{true}} \right| \times 100\% \qquad (14)$$

where P_{iden} and P_{true} are the identified parameter and the true parameter, respectively. Using this definition, the identification errors were calculated and the results are given in Table 3.

From Table 3, it can be seen that a satisfactory accuracy was achieved with most errors well below two percent. However, it was found that there are several cases with large identification errors and that these large errors seem to occur at high vehicle speeds. For example, for Truck 3 traveling at 30 m/s, the maximum error of axle spacing reaches 97.1 percent, indicating a failure of identification. The reason for these large errors is that some high-frequency information of the signal is lost due to the relatively low sampling frequency as the vehicle travels at a high speed. It will be shown in the next section that once the sampling frequency is increased, these errors will considerably decrease.

The successful axle identification using bridge global responses has significant implications since the vehicle speed and axle spacing can be identified using only the weighing sensors. In the real application, the use of this advanced axle detection technique will reduce the number of sensors to be installed and thus the cost of BWIM systems. Furthermore, since the identification

Table 2. Identified results using wavelet transformation.

Truck number	Number of axles	Identified results Velocity (m/s)	Axle spacing. First to second (m)	Axle spacing. Second to third (m)	Axle spacing. Third to fourth (m)	Axle spacing. Fourth to fifth (m)
1	2	9.93	6.21	N.A.	N.A.	N.A.
2	3	9.92	4.24	4.22	N.A.	N.A.
3	3	9.93	4.86	1.42	N.A.	N.A.
4	5	9.92	7.96	4.94	1.99	4.94
1	2	19.86	6.21	N.A.	N.A.	N.A.
2	3	19.85	4.22	4.27	N.A.	N.A.
3	3	19.85	4.67	1.64	N.A.	N.A.
4	5	19.89	7.96	5.07	1.94	4.92
1	2	29.92	6.28	N.A.	N.A.	N.A.
2	3	29.92	4.19	4.34	N.A.	N.A.
3	3	29.86	6.19	2.76	N.A.	N.A.
4	5	29.88	7.92	4.48	2.39	4.78

Table 3. Identification errors using wavelet transformation.

Truck number	Number of axles	Vehicle speed (m/s)	Identification errors (%) Velocity	Axle spacing. First to second	Axle spacing. Second to third	Axle spacing. Third to forth	Axle spacing. Fourth to fifth
1	2	10	0.70	0.64	N.A.	N.A.	N.A.
2	3	10	0.80	0.70	1.17	N.A.	N.A.
3	3	10	0.70	1.62	1.43	N.A.	N.A.
4	5	10	0.80	0.50	1.20	0.50	1.20
1	2	20	0.70	0.64	N.A.	N.A.	N.A.
2	3	20	0.75	1.17	0.00	N.A.	N.A.
3	3	20	0.75	5.47	17.1	N.A.	N.A.
4	5	20	0.55	0.50	1.40	3.00	1.60
1	2	30	0.27	0.48	N.A.	N.A.	N.A.
2	3	30	0.27	1.87	1.64	N.A.	N.A.
3	3	30	0.47	25.3	97.1	N.A.	N.A.
4	5	30	0.40	1.00	10.4	19.5	4.40

principle of this technique does not impose any restrictions on bridge types as in the case of FAD applications, it could potentially help extend the application of the BWIM technology to different types of bridges.

3.5. Parametric study

3.5.1. Effect of sampling frequency. As mentioned earlier, some large errors occurred due to the relatively low sampling frequency. To investigate the effect of sampling frequency on the identification accuracy, two sampling frequencies, i.e., 200 Hz and 500 Hz, are used to record the strain response for Truck 3 traveling at 30 m/s. Figure 7 shows the transformed signals under the two sampling frequencies. It should be mentioned that with the increase of sampling frequency, the scale of wavelet coefficients used for identification is reduced to 4.

From Figure 7, it can be clearly seen that the peaks in the transformed signal corresponding to the sampling frequency of 500 Hz are much sharper than the one corresponding to the sampling frequency of 200 Hz. As a result, the identified vehicle speed and the two axle spacings using the sampling frequency of

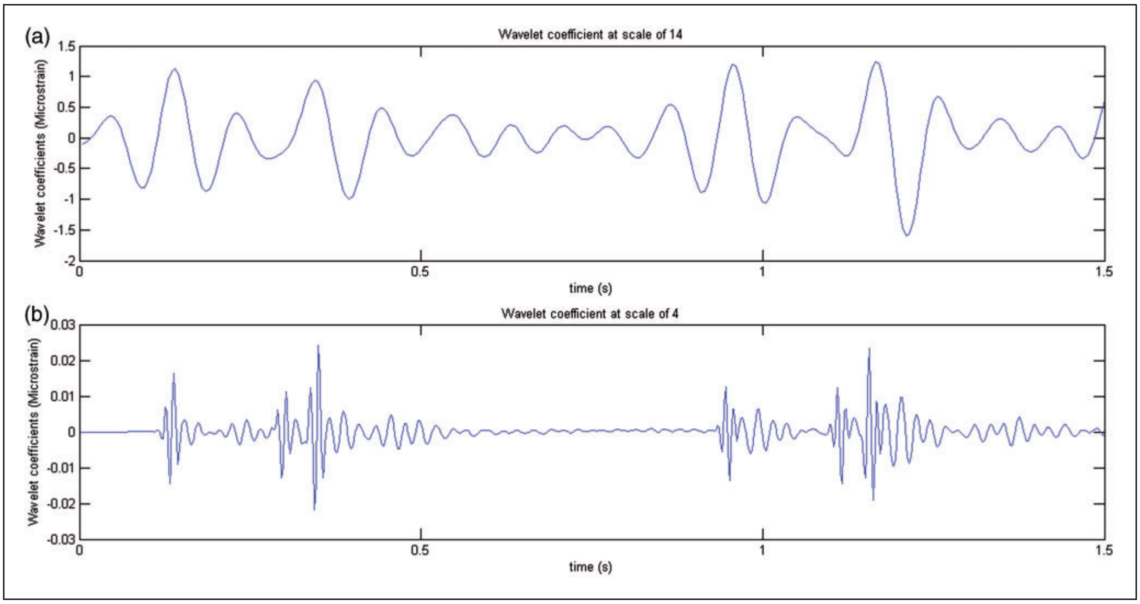

Figure 7. Wavelet transformations of signals for Truck 3 traveling at 30 m/s: (a) sampling frequency of 200 Hz and (b) sampling frequency of 500 Hz.

500 Hz changed to 30.25 m/s, 4.95 m and 1.42 m, respectively, and corresponding identification errors for the two axle spacings were reduced from 25.3% and 97.1% to 0.20% and 1.43%, respectively. For other cases with relatively large errors, it was also found that increasing the sampling frequency considerably reduced the identification errors.

Essentially, increasing the sampling frequency sharpens the peaks in the transformed signal, which, in turn, increases the accuracy of identification. However, higher sampling frequency would also substantially increase the amount of data and its processing time. Therefore, an appropriate sampling frequency should be determined based on the maximum vehicle speed of interest. In addition, this example also demonstrates that the wavelet analysis is capable of identifying closely-spaced axles which can be difficult sometimes for the FAD techniques (Chatterjee et al., 2006).

3.5.2. Effect of road surface condition. A road profile is usually represented by a zero-mean stationary stochastic process that can be expressed by a power spectral density (PSD) function. In this study, a modified PSD function (Wang and Huang, 1992) was used:

$$\varphi(n) = \varphi(n_0)\left(\frac{n}{n_0}\right)^{-2} \quad (n_1 < n < n_2) \tag{15}$$

where n is the spatial frequency (cycle/m); n_0 is the discontinuity frequency of 0.5π (cycle/m); $\varphi(n_0)$ is the roughness coefficient (m^3/cycle); and n_1 and n_2 are the lower and upper cut-off frequencies, respectively. The International Organization for Standardization (ISO, 1995) classified the road surface condition into several categories depending on different values of roughness coefficients. In the present study, according to ISO specifications (ISO, 1995), the roughness coefficients of 5×10^{-6}, 20×10^{-6}, 80×10^{-6}, and 256×10^{-6} m^3/cycle were used for very good, good, average, and poor road surface conditions, respectively.

The road surface elevation can then be generated by an inverse Fourier transformation as:

$$r(x) = \sum_{k=1}^{N} \sqrt{2\varphi(n_k)\Delta n}\cos(2\pi n_k x + \theta_k) \tag{16}$$

where θ_k is the random phase angle uniformly distributed between 0 and 2π; n_k is the wave number (cycle/m); N is the number of frequencies between n_1 and n_2; and Δn is the frequency interval between n_1 and n_2.

In order to examine the effect of road surface roughness on the identification accuracy, Truck 2 is set to travel at 20 m/s under four different surface conditions, i.e., very good, good, average, and poor road surface conditions and the sampling frequency is chosen to be 500 Hz. The wavelet transformations of the strain signals at the scale of 4 are presented in Figure 8. It can be seen that as the road roughness increases, the peaks used to identify the axles become less pronounced as there appears to have many other "noise" peaks. These other "noise" peaks are caused by the dynamic effect of

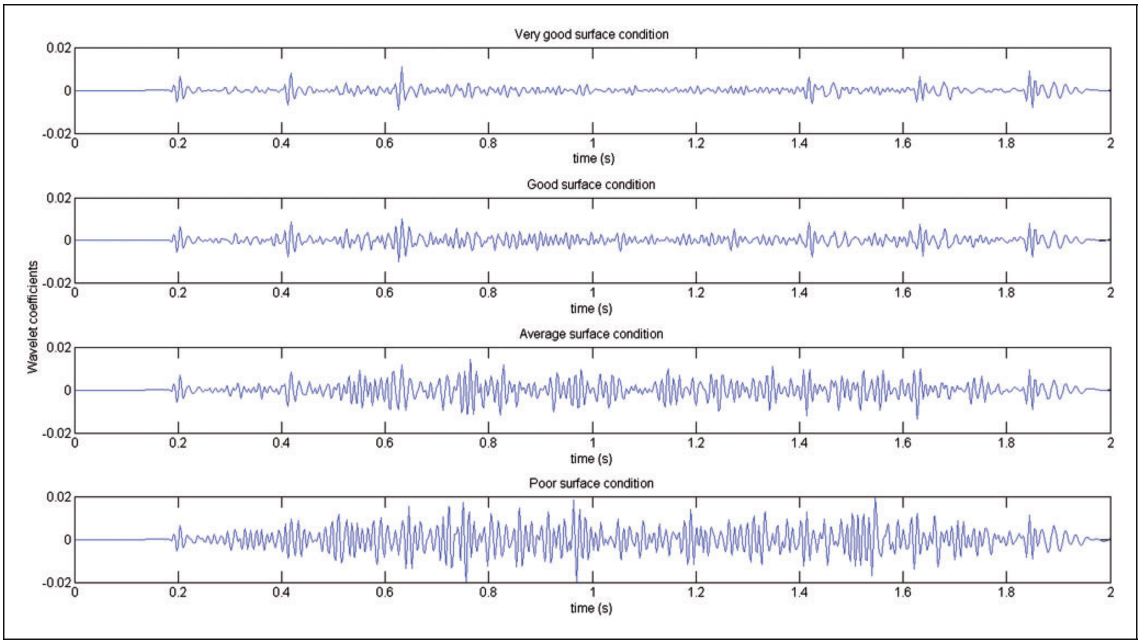

Figure 8. Wavelet transformations of signals under different road surface conditions.

the vehicle-bridge interaction. As the road surface condition worsens, these ''noise'' peaks become more pronounced, making the identification more difficult. Nevertheless, under very good and good surface conditions, the identification is still effective, as the identification errors were calculated to be below one percent. However, as road surface condition further deteriorates, the identification becomes infeasible since it is difficult to distinguish the peaks due to vehicle axles from other ''noise'' peaks caused by the dynamic effect.

In some previous studies on the bridge dynamic behaviors (e.g., Calçada et al., 2005, Ashebo et al., 2007), a low-pass filter was often employed to remove the dynamic effect of the response. However, in the case of axle identifications using wavelet analysis, low-pass filtering is not a solution, since the high frequency components of the signal contain the useful information used to identify the vehicle axles. Namely, low-pass filtering will also filter out the useful information. Nonetheless, it should be pointed out that, a smooth road condition is a prerequisite to achieve a satisfactory identification accuracy for most existing BWIM technologies such as those using Moses's algorithm (Moses, 1979, WAVE, 2001). Therefore, the fact that the axle identification using wavelet analysis is limited to good bridge surface conditions does not really impede the implementation of modern commercial BWIM systems whose basic framework is the Moses's algorithm (Moses, 1979). Naturally, a new methodology that can work well under rough road surface conditions, and at the same time can eliminate the axle detection sensors, is very desirable.

3.5.3. Effect of measurement noise. While the presented identified results above can be very accurate for good road surface conditions, they are obtained in the ideal situation. In real practice, the obtained signals are usually contaminated by measurement noises induced by the environmental changes and electric devices used for data acquisition. Thus, it is necessary to examine the effect of measurement noise on the identification accuracy. For this purpose, different levels of Gaussian white noise are added to the original strain signal obtained when Truck 2 travels at 20 m/s under sampling frequencies of 500 Hz and 200 Hz. As mentioned before, the scale of the wavelet coefficients for the two frequencies are 4 and 14, respectively. Figure 9 shows the wavelet transformations of the original signal and polluted signals under four different signal-to-noise ratios (SNR) of 100, 50, 20 and 10.

From Figure 9(a), it can be seen that under the sampling frequency of 500 Hz, the peaks induced by the vehicle axles quickly get submerged by the noise as the noise level increases, making the identification impossible. This suggests that the identification method is sensitive to the measurement noise. The main reason for this is that the information of vehicle axles is reflected by very delicate changes in the original signal. Therefore, it becomes very difficult to separate this information from the measurement noises even through de-noising techniques that allow the preservation of certain features of the original signal, such as median filter and wavelet de-noising.

Nevertheless, it was also noticed from Figure 9(b) that as the sampling frequency decreases to 200 Hz, the peaks induced by the vehicle axles tend to get submerged more slowly than the previous case, i.e., the identification becomes less susceptible to the noise under a lower sampling frequency. This is because while the scale of the noise remains the same, the scale of the peaks increased due to the lower sampling frequency. From this perspective, increasing the sampling frequency, though it sharpens the peaks induced by the vehicle axles, it does not necessarily increase the identification accuracy. Therefore, the choice of an optimal sampling frequency should take into consideration the maximum vehicle speed of interest as well as the level of noise.

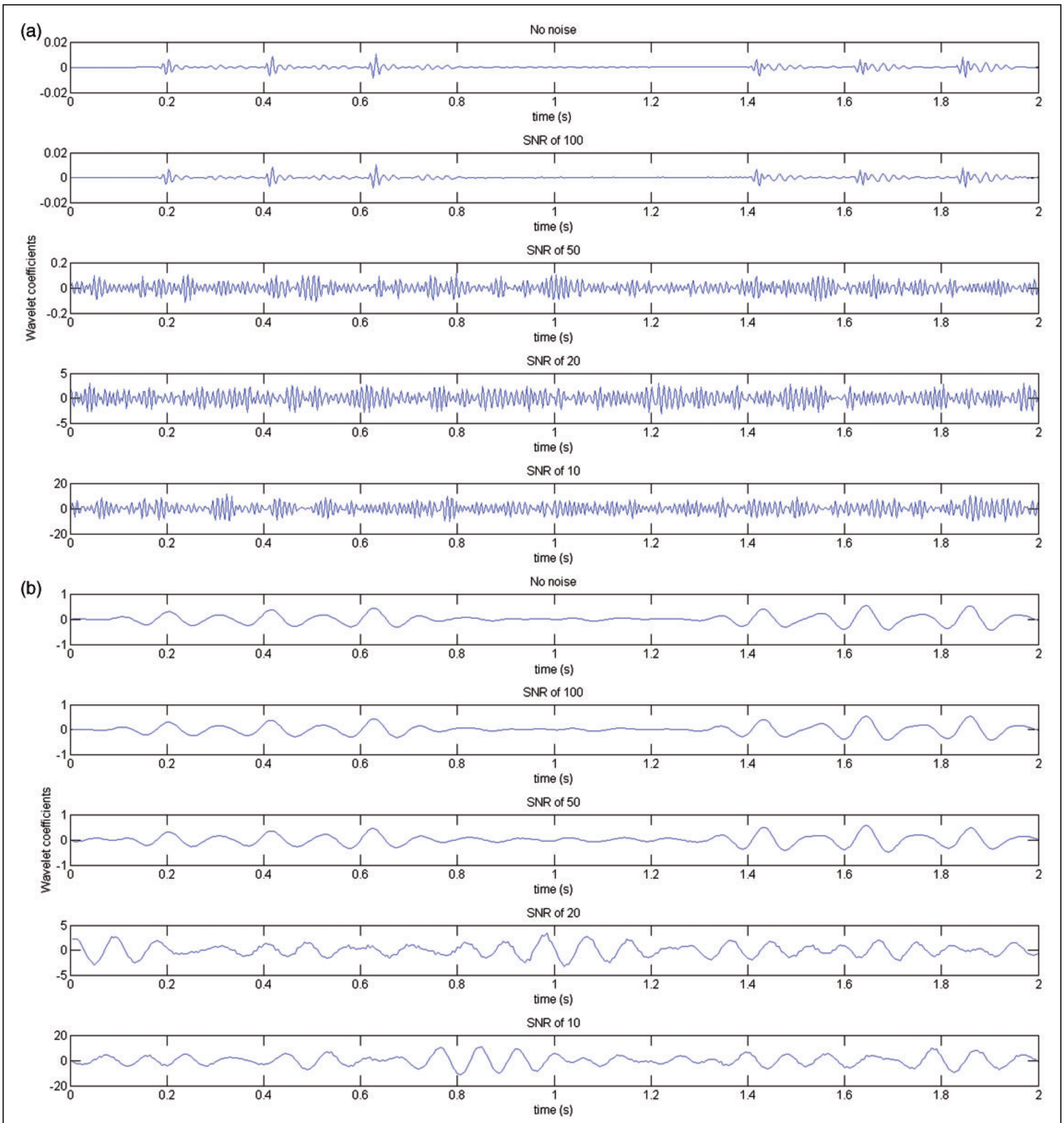

Figure 9. Wavelet transformations of signals under different levels of noise: (a) sampling frequency of 500 Hz and (b) sampling frequency of 200 Hz.

4. Concluding remarks

This paper presents a vehicle axle identification method using bridge global responses. The identification is achieved using a continuous wavelet transformation. Numerical simulations were conducted using three-dimensional vehicle and bridge models and the effect of several parameters including sampling frequency, road surface condition and measurement noise on the identification accuracy were investigated and discussed. Based on the results obtained, the following conclusions can be drawn:

1. Vehicle axle identifications can be achieved through a wavelet analysis of bridge global responses. This approach has obvious advantages over existing axle identification methods in that it requires fewer sensors and it does not impose any additional restrictions on the basis of the Moses's algorithm (Moses, 1979).
2. The sampling frequency of the data acquisition system has significant influence on the identification accuracy. A higher sampling frequency leads to sharper peaks in the transformed signal, which in turn, increases the identification accuracy, especially in cases where vehicles travel at relatively higher speeds.
3. Road surface condition also affects the accuracy of the axle identification in that road surface roughness causes additional peaks in the transformed signal due to the vehicle-bridge interaction, and once these peaks overcome the peaks induced by the vehicle axles, the identification of vehicle axles becomes very difficult.
4. The proposed identification method is susceptible to measurement noises. This is inevitable since the information on vehicle axles is reflected by very delicate changes in the original signal. Nevertheless, it has been shown that reducing the sampling frequency increases the scale of the peaks induced by the vehicle axles and thus makes the identification less susceptible to the measurement noise.

While the proposed method in this paper provides a promising tool for the axle identification of BWIM systems, limitations and conditions are also recognized and noted. Future work will be conducted to experimentally verify this method and relevant algorithms will be designed to enable automatic identification of vehicle axles in the BWIM systems.

Acknowledgments

We would like to express thanks to the project manager Dr. Walid Alaywan and those who provided help during the development of this research program.

Declaration of Conflicting Interests

The author(s) declared no potential conflicts of interest with respect to the research, authorship, and/or publication of this article.

Funding

The author(s) disclosed receipt of the following financial support for the research, authorship, and/or publication of this article: financial support was provided by the Louisiana Transportation and Research Center (No. 13-2ST).

References

American Association of State Highway and Transportation Officials (AASHTO) (2002) *Standard specifications for highway bridges*. Washington, USA.

Ashebo DB, Chan THT and Yu L (2007) Evaluation of dynamic loads on a skew box girder continuous bridge Part II: Parametric study and dynamic load factor. *Engineering Structures* 29: 1064–1073.

Broquet C, Bailey S, Fafard M and Brühwiler E (2004) Dynamic behavior of deck slabs of concrete road bridges. *Journal of Bridge Engineering* 9: 137–146.

Calçada R, Cunha A and Delgado R (2005) Analysis of traffic-induced vibrations in a cable-stayed bridge. Part I: Experimental assessment. *Journal of Bridge Engineering* 10: 370–385.

Chatterjee P, O'Brien EJ, Li Y and Gonzales A (2006) Wavelet domain analysis for identification of vehicle axles from bridge measurements. *Computers and Structures* 84: 1792–1801.

Deng L and Cai CS (2010) Development of dynamic impact factor for performance evaluation of existing multi-girder concrete bridges. *Engineering Structures* 32: 21–31.

Dunne D, O'Brien EJ, Basu B and González A. (2005) Bridge WIM systems with nothing on the road (NOR). *Proceedings of the 4th International WIM Conference*, Taipei, China.

Gabor D (1946) Theory of communication. *Journal of the Institution of Electrical Engineers* 93: 429–457.

International Organization for Standardization (ISO) (1995). *Mechanical vibration-road surface profiles–reporting of measured data*. ISO 8608: 1995(E). Geneva: ISO.

Moses F (1979) Weigh-in-motion system using instrumented bridges. *Transportation Engineering Journal of ASCE* 105: 233–249.

O'Brien EJ, Znidaric A and Dempsey AT (1999) Comparison of two independently developed bridge weigh-in-motion systems. *International Journal of Heavy Vehicle Systems* 6: 147–161.

Quilligan M (2003) Bridge Weigh-in-Motion: Development of a 2-D multi-vehicle algorithm. *Trita-BKN. Bulletin* 69: A–144.

Wang T and Huang D (1992) Cable-stayed bridge vibration due to road surface roughness. *Journal of Structural Engineering* 118: 1354–1374.

WAVE (2001) *Weighing-in-motion of axles and vehicles for Europe (WAVE): Report of Work Package 1.2* O'Brien EJ and Znidaric A (eds) Dublin: University College Dublin.